Synthesis and crystal structure of a silver(I) 6-methylmercaptopurine riboside complex

Authors

Lamia L. G. Al-Mahamad[a]* and William Clegg[b]

[a]Department of Chemistry, College of Science, Mustansiriyah University, Baghdad, Iraq

[b]School of Natural and Environmental Sciences, Newcastle University, Newcastle upon Tyne, NE1 7RU, United Kingdom

Correspondence email: lamia.al-mahamad@yahoo.com

Funding information Iraqi Ministry of Higher Education and Scientific Research (scholarship No. no number available to Lamia L. G. Al-Mahamad); Diamond Light Source (award No. MT11145 to William Clegg).

Synopsis Silver has an almost linear primary coordination with two N-bound ligands, the nitrate anion giving weaker secondary coordination in a bidentate mode.

Abstract Silver nitrate reacts with 6-methylmercaptopurine riboside (6-MMPR) in aqueous solution containing methanol and DMSO at room temperature to give a colourless crystalline complex. The crystal structure, determined from synchrotron diffraction data, shows a central Ag(I) ion on a crystallographic twofold rotation axis, coordinated in an almost linear fashion by two 6-MMPR ligands via N7, with the nitrate counterion loosely coordinated as a bidentate ligand, forming a discrete molecular complex as an approximate dihydrate. The complex and the water molecules are connected in a three-dimensional network by hydrogen bonding.

Keywords: crystal structure; silver complex; thiopurine; riboside; secondary coordination

Introduction

6-Methylmercaptopurine riboside [6-MMPR; also known as methylthioinosine, IUPAC (2*R*,3*S*,4*R*,5*R*)-2-(hydroxymethyl)-5-(6-methylsulfanylpurin-9-yl)oxolane-3,4-diol] belongs to the class of thiopurines, purine analogues that derive from natural bases and nucleosides. This class includes 6-mercaptopurine and azathioprine, which are medical treatments for cancer and immune system problems. 6-Thiopurine nucleosides have attracted much attention

due to their broad activity as antitumour agents (Elion, 1989; O'Dwyer *et al*., 1991; Redei *et al*., 1994; Gupta *et al*., 1988), and very recently 6-MMPR has shown a promising antiviral activity against Zika virus, as it was able to reduce virus production by up to 99% (de Carvalho *et al*., 2017*a*). Another study showed that 6-MMPR has antiviral activity against canine distemper virus (CDV) (de Carvalho *et al*., 2017*b*). Numerous reports have described the bioactivity of this compound (Volonté & Greene, 1992; Presta *et al*., 1999; Wong *et al*., 2017; Chrzanowska *et al*., 1999). The reactions of metal ions with nucleobase and nucleoside molecules can give products with diverse structures, as these molecules have a range of possible binding sites and, consequently, the resulting complexes display specific properties according to the binding mode (Amo-Ochoa *et al*., 2014; Amo-Ochoa *et al*., 2013), such as luminescence (Purohit & Verma, 2006; Jonckheere *et al*., 2016), electronic features (Delgado *et al*., 2008), catalysis (Verma *et al*., 2010), and gas adsorption (Pérez-Yáñez *et al*., 2011). In addition, complexes of this kind have found special applications in the medical field (Das & Livingstone, 1978; Yamanari *et al*., 1996; Shen *et al*., 1966; Ansari *et al*., 2010). On the other hand, substitution of O6 by sulfur in these nucleobase and nucleoside compounds leads to hydrogels with coinage metal ions (Cu, Ag, and Au), and this gives the possibility of using these materials in different applications according to their physicochemical properties.

The most common metal binding site in purine is N7, while N3 is considered a rare single binding site (Aoki *et al*., 2016; Lippert, 2000; Leonarski *et al*., 2016). Complexes of Na^+ and K^+ with 9-ethyladenine and 18-aza-crown have been prepared, and the coordination of the metal ions by the ligand occurs via N3 (Gibson *et al*., 2002). It was also found that Cu(I) and Ag(I) ions can bind to the dithioether of adenine via N3 (Galindo *et al*., 2009a). Metal ions including Li^+, Na^+, K^+, and Cs^+ can be coordinated by adenine via N3 and N9 atoms (Rajabi *et al*., 2010). Numerous complexes (Bu *et al*., 2002; Bu *et al*., 2003; Sun *et al*., 2012) were prepared by the reaction of aliphatic or aromatic thioethers with different metal ions, e.g, the reaction of thianthrene (TA) with $AuCl_3$ in the presence of liquid $SOCl_2$ (Tjahjanto & Beck, 2009); the product was a black crystalline solid with square-planar geometry for both ions, dichloridobis(thianthrene)gold(III) tetrachloridoaurate(III). Cu(I) is coordinated by two (1-(N9-adenine)-3,6-dithiaheptane) ligands via four S atoms to form a complex that contains two adenine residues (Galindo *et al*., 2009b). Recently a complex Zn with 6-MMP (6-methylmercaptopurine) was prepared by Perea-Cachero *et al*. (2016); it is a two-dimensional polymer with Zn atoms that act as bridges between the ligands via N atoms at the positions N9 and N7.

We have found no report in the literature involving the reaction of metal ions with 6-MMPR. Interestingly, the reaction of coinage metal ions with 6-mercaptopurine and 6-mercaptopurine riboside produced hydrogels rather than crystalline compounds, and this may be due to the effect of the methyl substituent on S6 (Al-Mahamad, 2017). In addition, the reaction of 2-amino-6-mercaptopurine and 2-amino-6-mercaptopurine riboside with elements of group 11 also produced hydrogels (Al-Mahamad *et al*., 2017; Al-Mahamad, 2019, 2020; El-Zubir *et al*., 2022). We report here that a crystalline product is obtained from the reaction of Ag(I) with 6-MMPR, the structure of which has been determined with synchrotron radiation from a very small crystal.

Experimental

All chemicals were purchased from Sigma Aldrich and were used as received. Deionized water was obtained from Nanopure purification system, Barnstead, with a nominal resistivity of 18 MΩ cm).

A solution of $AgNO_3$ (0.0569 g, 0.0335 mmol) in 400 μL MeOH and 1.6 mL H_2O was added to a solution of 6-MMPR (0.1 g, 0.0335 mmol) in 2 mL DMSO, 2 mL MeOH and 4 mL H_2O. The two solutions were mixed gently, and small colourless crystals were formed after 5 min. The reaction mixture was left in the dark for 3h, then the crystals were filtered off, washed with water, and left to dry in the air. The product was recrystallised using 1:1 MeOH-H_2O then filtered and dried again in the air (yield 0.075 g, 75% with respect to the ligand). Analysis, found: C 32.96, H 3.23, N 15.75%; $C_{22}H_{32}AgN_8O_8S_2$ requires C 32.92, H 3.98, N 15.71%. Investigation of the morphology of the crystalline product with SEM showed a lath-like elongated tabular habit of regular form and varied but small size (Supporting Information).

IR spectra were obtained from solid samples with a Varian 800 FT-IR instrument in transmittance mode in the range 400 to 4000 cm^{-1}. A Cary 100 Bio UV-Visible spectrophotometer provided measurements at room temperature in the wavelength range 200–600 nm using a quartz cuvette. Elemental analysis (CHN) was carried out using a Carlo Erba 1108 Elemental Analyser controlled with CE Eager 200 software. Spectroscopic data are given in the Supporting Information.

Crystals were found to be composite and weakly diffracting. Single-crystal diffraction data were collected at beamline I19 of Diamond Light Source and intensities were extracted from the composite pattern for the dominant major component. Data quality was sufficient to enable refinement of hydroxy and ordered water H atoms with soft distance restraints and

unconstrained individual isotropic displacement parameters; standard constraints were applied to C-bonded H atoms. The structure is fully ordered except for partial occupancy of an interstitial site by water disordered across a twofold rotation axis. Refinement gives an occupancy of 0.157(9) at each of two sites separated by 0.85 Å, corresponding to an increase of approximately $0.3H_2O$ above the notional dihydrate formulation for the complex. The disorder and low occupancy preclude modelling of H atoms for this additional water, but it forms short O…O contacts of approximately 2.5 Å with the nitrate O22, which is otherwise not involved in hydrogen bonding. Inclusion of the disordered water gives a significant reduction in residual indices (*R* and *wR*) and a maximum residual electron density peak of 0.62 instead of 1.35 e $Å^{-3}$.

Results and discussion

The silver complex crystallises in the non-centrosymmetric space group $C222_1$, consistent with the enantiopure chirality of the 6-MMPR ligand (2*R*,3*S*,4*R*,5*R* absolute configuration for the ribose unit). The Ag(I) ion, coordinated by two 6-MMPR ligands, lies on a crystallographic twofold rotation axis, so the two ligands are symmetry-equivalent. Coordination of 6-MMPR occurs through N7, the mostly commonly observed metal-binding site for purine derivatives; the Ag–N bond length is 2.156(3) Å and the N–Ag–N angle is 164.03(13)°, deviating only 16° from linearity. This slight bending is caused by the weak coordination of the nitrate counterion in bidentate mode, with two Ag–O bonds of length 2.630(3)Å and an O–Ag–O angle of 48.91(16)°. Coordination of the nitrate has little effect on its internal geometry, with the metal-bound N–O bonds only 0.024 Å longer than the uncoordinated N–O [1.263(4) and 1.239(5) Å, respectively], and angles at N deviating only slightly from 120° [two of 120.5(2)° and one of 119.0(4)°]. The loosely associated cation and anion thus form a discrete mononuclear uncharged molecular species (Figure 1). These molecules and uncoordinated water molecules (stoichiometrically an approximate dihydrate with 2.3 water molecules per complex molecule) are connected by hydrogen bonding, in which all the ribose OH groups and the ordered water molecules serve as donors and the acceptors are water and coordinated nitrate O atoms, one of the ribose OH O atoms, and the unsubstituted N atoms (N1 and N3) of the purine residue. The hydrogen bonding interactions generate a three-dimensional network (Figure 2).

A search of the Cambridge Structural Database (CSD) (Groom *et al*., 2016) for silver(I) complexes of purine derivatives yields around 40 structures, 23 of which contain nitrate as a counterion. In nine of these the nitrate is uncoordinated (Pandey *et al*., 2010; Venkatesh *et al*., 2011; Mishra *et al*., 2010; Prajapati *et al.*, 2013; Purohit & Verma, 2006; Gagnon & Beauchamp, 1977; Mishra *et al*., 2008; Menzer *et al*., 1992; Rother *et al*., 2002). Eight feature nitrate as a monodentate ligand coordinated to Ag through one O atom (Mirshra *et al*., 2010; Sinha *et al*., 2013; Purohit *et al*., 2007; Sinha *et al*., 2016; Clegg & Harrington, 2020; Kumar *et al*., 2016). One structure has nitrate as a 1,3 O–N–O bridge between pairs of metal centres with the third O atom uncoordinated (Purohit & Verma, 2007), while Ag–O–Ag bridges are found in another together with terminal monodentate nitrate ligands (Mishra *et al*., 2010). A few structures display two of these functions for nitrate anions (Kumar *et al*., 2016; Mishra & Verma, 2010; Pratibha & Verma, 2015). There is only one previous example of a bidentate nitrate ligand (Mishra *et al*., 2013) (though there are several hundred cases with ligands other than purine derivatives); interestingly, this contains a 6-diethylaminopurine derivative coordinated unusually through N3 to give a discrete mononuclear uncharged molecular species with a very similar coordination geometry to that of the title silver complex.

The C–S stretching mode (Rao *et al*., 1964; Febretti *et al*., 1983) is found in the infrared spectra of both the ligand (632 cm^{-1}) and the complex (624 cm^{-1}), indicating that coordination does not occur through the S atom, as revealed by crystallography; the small difference in the frequency (8 cm^{-1}) can be ascribed to the change in the bond force constant upon coordination to the Ag(I) ion. The new bands at 1296 and 1381 cm^{-1} in the spectrum of the complex but not for the ligand can be assigned to N–O vibrations of a silver-coordinated nitrate anion (Kubota *et al*., 1966; Goel & Pilon, 1978), perturbed from that of the free nitrate anion as a result of splitting the asymmetric N–O stretching modes (Goel & Pilon, 1978; Senelaa *et al*., 2005; Li *et al*., 2008). The other new band at 516 cm^{-1} in the spectrum of the complex can be assigned to an asymmetric Ag–N stretching band (Kubota *et al*., 1966), as it was reported that such an arrangement of Ag–N bonds has two stretching bands: symmetric (usually found at about 380 cm^{-1}) and asymmetric (between 430 and 500 cm^{-1}) (Fabretti *et al*., 1983; Morzyk-Ociepa & Michalska, 2003; Geddes & Bottger, 1969). The stretching mode of C=N at 1442 cm^{-1} in the spectrum of the ligand is shifted to a slightly higher frequency for the complex (1450 cm^{-1}), suggesting that the coordination to Ag(I) takes place via N7. The band observed at 3741 cm^{-1} is due to the presence of uncoordinated water

molecules in the crystal structure (Mitev *et al*., 2015; Cheng *et al*., 2013; Lepodise *et al*., 2013; De Munno *et al*., 2000); the bending mode of H_2O (Rey *et al*., 2009; Elioff & Mullin, 2000) can be seen around 1660 cm^{-1}.

The UV-visible spectrum of 6-MMPR in methanol (Figure S3, SI) shows an absorption band at 290 nm that can be attributed to π–π* transitions (Zimmerman & Elion, 1974; Dervieux & Boulieu, 1998). No shift is seen in this band in the spectrum of the complex, and this indicates probable dissociation of the complex in solution.

Acknowledgements Lamia. L. G. Al-Mahamad acknowledges Professor Andrew Houlton and Dr Benjamin Horrocks of Newcastle University for research facilities.

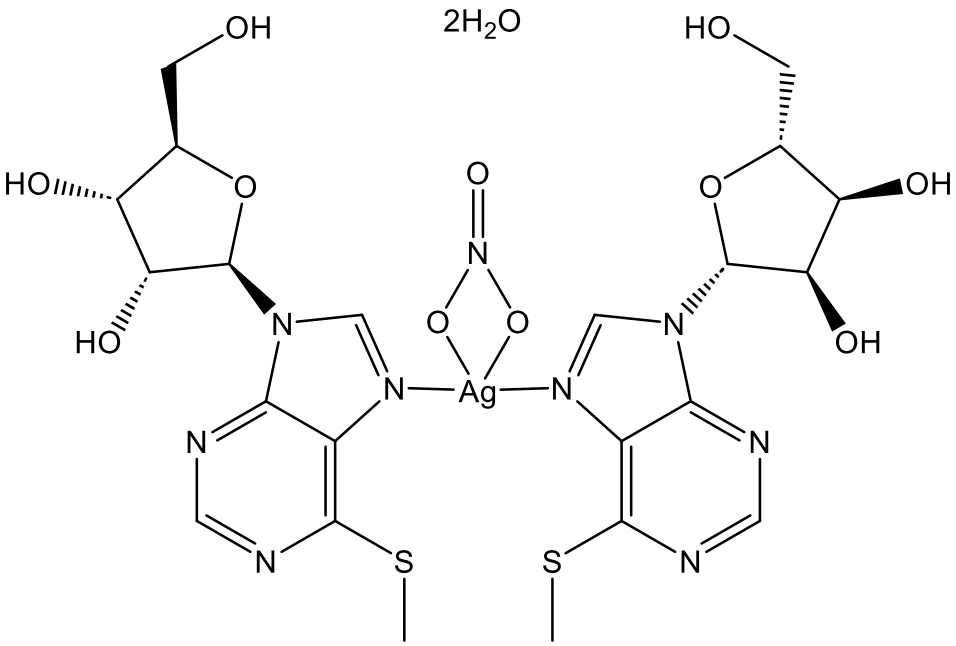

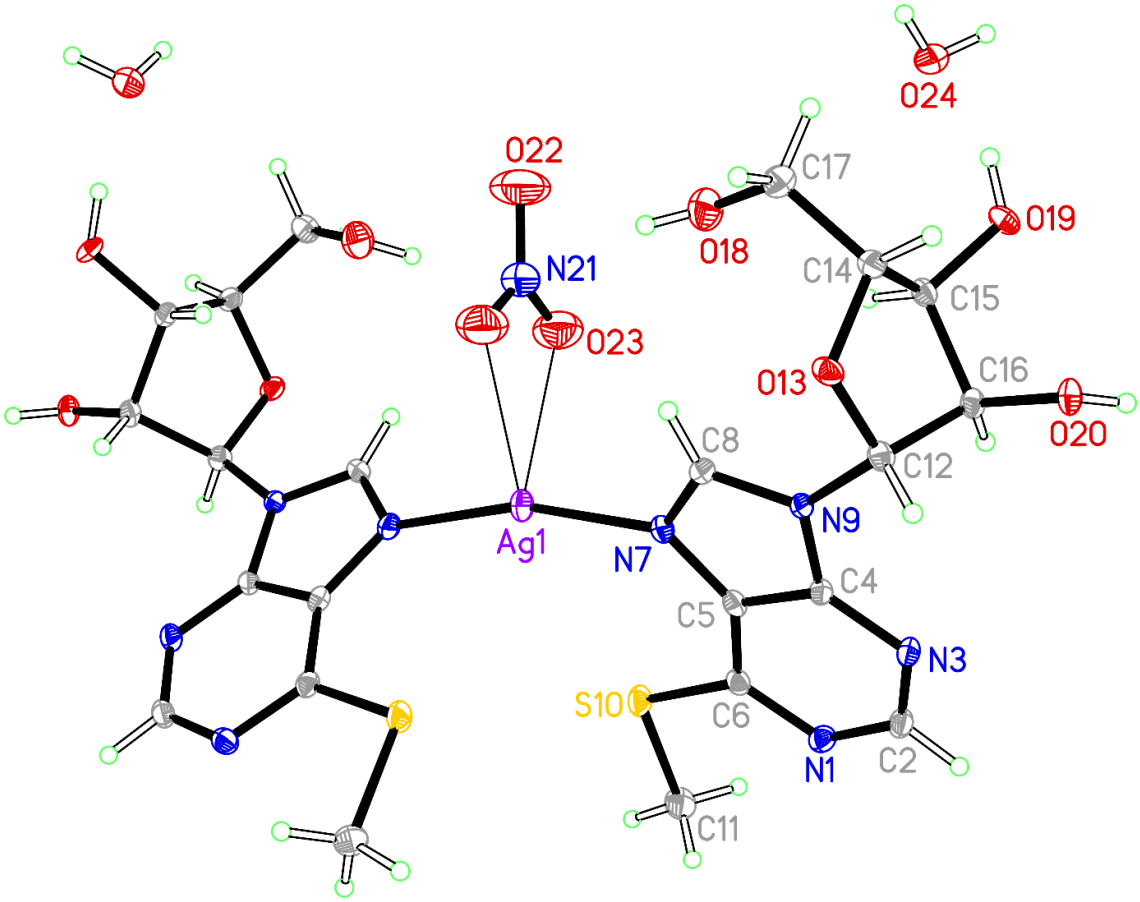

Figure 1 The molecular structure of the complex, having twofold rotation symmetry and with associated water molecules. Non-H atoms of the asymmetric unit are labelled.

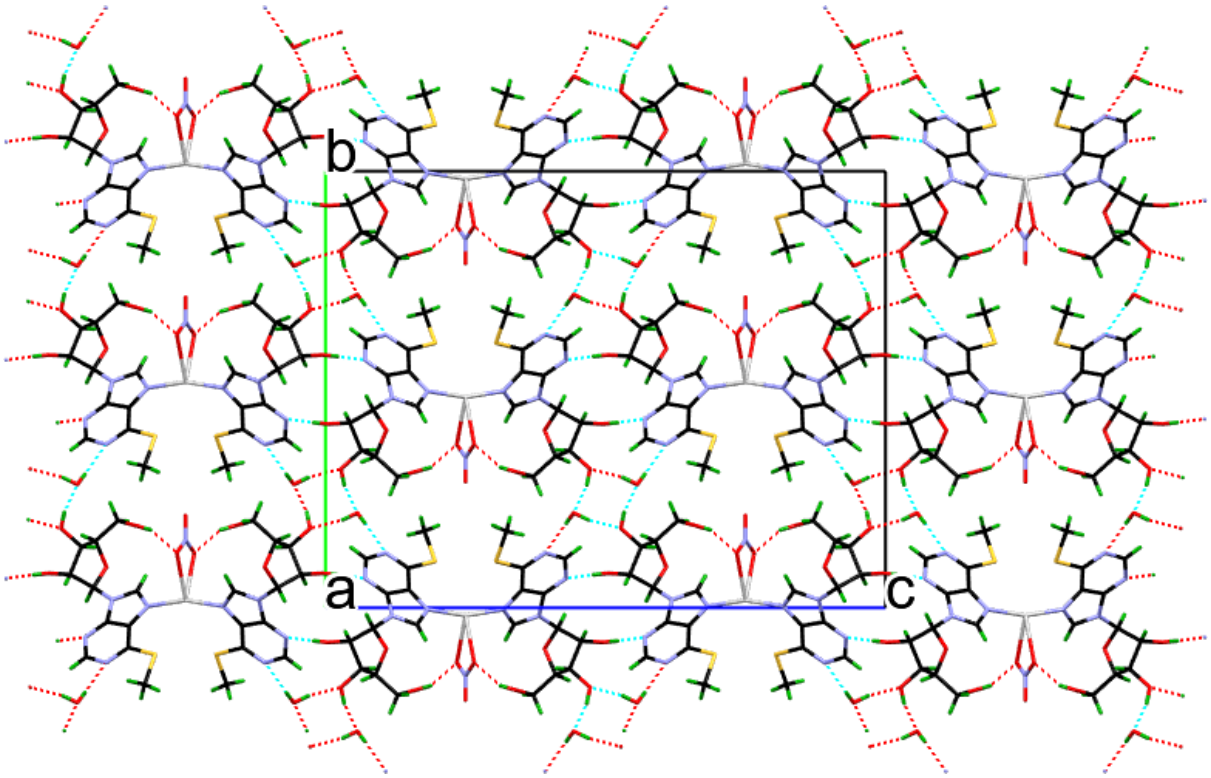

Figure 2. Network of hydrogen bonds in the crystal structure, viewed down the ***a*** axis.

Table 1 Experimental details

Crystal data	
Chemical formula	$C_{22}H_{28}AgN_8O_8S_2^+ \cdot NO_3^- \cdot 2.32H_2O$
M_r	808.23
Crystal system, space group	Orthorhombic, $C222_1$
Temperature (K)	100
a, b, c (Å)	4.8791 (10), 22.049 (5), 28.256 (6)
V (Å^3)	3039.8 (11)
Z	4
Radiation type	Synchrotron, λ = 0.6889 Å
μ (mm^{-1})	0.82
Crystal size (mm)	0.06 × 0.02 × 0.01
Data collection	
Diffractometer	Rigaku Saturn 724+ CCD on kappa diffractometer
Absorption correction	Multi-scan *SADABS* 2016/2: (Krause *et al.*, 2015)
T_{min}, T_{max}	0.734, 0.976
No. of measured, independent and observed [$I > 2\sigma(I)$] reflections	14892, 3672, 3410
R_{int}	0.045
$(\sin\theta/\lambda)_{max}$ (Å^{-1})	0.668
Refinement	
$R[F^2 > 2\sigma(F^2)]$, $wR(F^2)$, S	0.029, 0.068, 1.10
No. of reflections	3672
No. of parameters	245

No. of restraints	6
H-atom treatment	H atoms treated by a mixture of independent and constrained refinement
$\Delta\rho_{max}$, $\Delta\rho_{min}$ (e Å^{-3})	0.62, −0.53
Absolute structure	Flack x determined using 1339 quotients [(I+)-(I-)]/[(I+)+(I-)] (Parsons *et al*., 2013)
Absolute structure parameter	0.034 (13)

Computer programs: *CrystalClear* (Rigaku, 2008–2015), *APEX2* (Bruker, 2012), *SHELXT*-2014/4 (Sheldrick, 2015*a*), *SHELXL*-2019/2 (Sheldrick, 2015*b*), Bruker *SHELXTL* (Bruker, 2012) and local programs.

Table 2 Selected geometric parameters (Å, º) for (aho150019)

Ag1—N7	2.156 (3)	Ag1—O23	2.630 (3)
N7—Ag1—N7^{i}	164.03 (13)	N7^{i}—Ag1—O23	96.26 (10)
N7—Ag1—O23	98.27 (10)	O23—Ag1—O23^{i}	48.91 (16)

Symmetry code: (i) −*x*+1, *y*, −*z*+1/2.

Table 3 Hydrogen-bond geometry (Å, º) for (aho150019)

D—H···*A*	*D*—H	H···*A*	*D*···*A*	*D*—H···*A*
O18—H18···O23^{ii}	0.85 (1)	2.08 (2)	2.895 (4)	161 (5)
O19—H19···O24	0.83 (1)	1.86 (2)	2.674 (4)	167 (5)
O20—H20···N3^{iii}	0.84 (1)	2.00 (2)	2.812 (4)	163 (5)
O24—H24*A*···O19^{iv}	0.83 (1)	1.98 (2)	2.772 (4)	159 (4)
O24—H24*B*···N1^{v}	0.84 (1)	2.11 (2)	2.943 (4)	174 (5)

Symmetry codes: (ii) *x*+1, *y*, *z*; (iii) *x*, −*y*+1, −*z*+1; (iv) *x*−1/2, −*y*+1/2, −*z*+1; (v) *x*+1/2, *y*−1/2, *z*.

References

Al-Mahamad, A. L. G. (2017). PhD Thesis, Newcastle University.

Al-Mahamad, A. L. G. (2019). *Heliyon* **5**, e01609.

Al-Mahamad, A, L. G. (2020). Presented in part at the IEEE 10th International Conference on Nanomaterials: Applications and Properties (NAP), Sumy, Ukraine.

Al-Mahamad, A. L. G., El-Zubir, O., Smith, D. G., Horrocks, B. R. & Houlton, A. (2017). *Nat. Commun.* **8**, 720.

Amo-Ochoa, P., Castillo, O., Guijarro, A., Sanz Miguel, P. J. & Zamora, F. (2014). *Inorg. Chim. Acta*, 2014, **417**, 142–147.

Ansari, A., Patel, N., Sanderson, J., O'Donohue, J., Duley, J. A. & Florin, T. H. (2010). *Aliment. Pharmacol. Ther.* **31**, 640–647.

Aoki, K., Murayama, K. & Hu, N. H. (2016). *Met. Ions Life Sci.* **16**, 27–101.

Bruker (2012). *APEX2* and *SHELXTL*. Bruker AXS Inc., Madison, Wisconsin, USA.

Bu, X.-H., Chen, W., Du, M., Biradha, K., Wang, W.-Z. & Zhang, R.-H. (2002). *Inorg. Chem.* **41**, 437–439.

Bu, X.-H., Xie, Y.-B., Li, J.-R. & Zhang, R. H. (2003). *Inorg. Chem.* **42**, 7422–7430.

de Carvalho, O. V., Félix, D. M., de Camargo Tozato, C., Fietto, J. L. R., de Almeida, M. R., Bressan, G. C., Pena L. J. & Silva-Júnior, A. (2017a). *Virol. J.* **14**, 124.

de Carvalho, O. V., Félix, D. M., de Mendonça, L. R., de Araújo, C. M. C. S., de Oliveira Franca, R. F., Cordeiro, M. T., Silva-Júnior A. & Pena, L. J. (2017b). *Int. J. Antimicrob. Ag.* **50**, 718–725.

Chrzanowska, M., Kolecki, P., Duczmal-Cichocka, B. & Fiet, J. (1999). *Eur. J. Pharm. Sci.* **8**, 329–334.

Cheng, F., Cao, Q., Guan, Y., Cheng, H., Wang, X. & Miller, J. D. (2013). *Int. J. Miner. Process.* **122**, 36–42.

Clegg, W. & Harrington, R. W. (2020). *CSD Commun.* NUVQIH

Das, M. & Livingstone, S. E. (1978). *Br. J. Cancer* **38**, 325–328.

Delgado, S., Sanz Miguel, P. J., Priego, Jiménez-Aparicio, R., Gómez-García, C. J. & Zamora, F. (2008). *Inorg. Chem.* **47**, 9128–9130.

De Munno, G., Medaglia, M., Armentano, D., Anastassopoulou, J. & Theophanides, T. (2000). *J. Chem. Soc., Dalton Trans.* pp. 1625–1629.

Dervieux, T. & Boulieu, R. (1998). *Clin. Chem.* **44**, 2511–2515.

Elioff, M. S. & Mullin, A. S. (2000). *J. Phys. Chem. A* **104**, 10304–10311.

Elion, G. B. (1989). *Science* **244**, 41–47.

El-Zubir, O., Martinez, P. R., Dura, G., Al-Mahamad, L. L. G., Pope, T., Penfold, T. J., Mackenzie, L. E., Pal, R., Mosely, J., Cucinotta, F., McGarry, L. F., Horrocks, B. R. & Houlton, A. (2022). *J. Mater. Chem. C* **10**, 7329–7335.

Fabretti, A. C., Peyronel, G., Giusti A. & Zanoli, A. F. (1983). *Polyhedron* **2**, 475–477.

Gagnon, C. & Beauchamp, A. L. (1977). *Acta Cryst.* B**33**, 1448–1454.

Galindo, M. A., Amantia, D., Clegg, W., Harrington, R. W., Eyre, R. J., Goss, J. P., Briddon, P. R., McFarlane, W. & Houlton, A. (2009a). *Chem. Commun.* pp. 2833–2835.

Galindo, M. A., Amantia, D., Martinez Martinez, A., Clegg, W., Harrington, R. W., Moreno Martinez, V. & Houlton, A. (2009b). *Inorg. Chem.* **48**, 10295–10303.

Geddes, A. L. & Bottger, G. L. (1969). *Inorg. Chem.* **8**, 802–807.

Gibson, A. E., Price, C., Clegg, W. & Houlton, A. (2002). *J. Chem. Soc., Dalton Trans.* pp. 131–133.

Goel, R. G. & Pilon, P. (1978). *Inorg. Chem.* **17**, 2876–2879.

Groom, C. R., Bruno, I. J., Lightfoot, M. P. & Ward, S. C. (2016). *Acta Cryst.* B**72**, 171–179.

Gupta, R. S., Murray, W. & Gupta, G. (1988). *Brit. J. Cancer* **58**, 441–447.

Jonckheere, D., Coutino-Gonzalez, E., Baekelant, W., Bueken, B., Reinsch, H., Stassen, I., Fenwick, O., Richard, F., Samorì, P., Ameloot, R., Hofkens, J., Roeffaers, M. B. J. & De Vos, D. E. (2016). *J. Mater. Chem. C*, **4**, 4259–4268.

Krause, L., Herbst-Irmer, R., Sheldrick, G. M. & Stalke, D. (2015). *J. Appl. Cryst.* **48**, 3–10.

Kubota, M., Johnston, D. L. & Matsubara, I. (1966). *Inorg. Chem.* **5**, 386–391.

Kumar, J., Pratibha & Verma, S. (2016). *Inorg. Chim. Acta* **452**, 214–221.

Leonarski, F., D'Ascenzo, L. & Auffinger, P. (2016). *Inorg. Chim. Acta* **452**, 82–89.

Lepodise, L. M., Horvat, J. & Lewis, R. A. (2013). *Phys. Chem. Chem. Phys.* **15**, 20252–20261.

Li, M. X., Miao, Z. X., Shao, M., Liang, S. W. & Zhu, S. R. (2008). *Inorg. Chem.* **47**, 4481–4489.

Lippert, B. (2000). *Coord. Chem. Rev.* **200**–**202**, 487–516.

Menzer, S., Sabat. M. & Lippert, B. (1992). *J. Am. Chem. Soc*. **114**, 4644–4649.

Mishra, A. K., Prajapati, R. K. & Verma, S. (2010). *Dalton Trans*. **39**, 10034–10037.

Mishra, A. K., Prajapati, R. K. & Verma, S. (2013). *Indian J. Chem. Sect. A* **52**, 1041–1046.

Mishra, A. K., Purohit, C. S. & Verma, S. *CrystEngComm* **10**, 1296–1298.

Mishra, A. K. & Verma, S. (2010). *Inorg. Chem*. **49**, 8012–8016.

Mitev, P. D., Eriksson, A., Boily, J.-F. & Hermansson, K. (2015). *Phys. Chem. Chem.Phys*. **17**, 10520–10531.

Morzyk-Ociepa, B. & Michalska, D. (2003). *Spectrochim. Acta A: Mol. Biomol. Spec.* **59**, 1247–1254.

O'Dwyer, P. J., Hudes, G. R., Colofiore, J., Walczak, J., Hoffman, J., LaCreta, F. P.; Comis, R. L., Martin, D. S. & Ozols, R. F. (1991). *J. Natl. Cancer I.* **83**, 1235–1240.

Pandey, M. D., Mishra, A. K., Chandrasekhar, V. & Verma, S. (2010). *Inorg. Chem*. **49**, 2020–2022.

Parsons, S., Flack, H. D. & Wagner, T. (2013). *Acta Cryst.* B**69**, 249–259.

Perea-Cachero, A., Seoane, B., Diosdado, B., Téllez, C. & Coronas, J. (2016). *RSC Adv*. **6**, 260–268.

Pérez-Yáñez, S., Beobide, G., Castillo, O., Cepeda, J., Luque, A., Aguayo, A. T. & Román, P. (2011). *Inorg. Chem.* **50**, 5330–5332.

Pratibha & Verma, S. (2015). *Cryst. Gr. Des.* **15**, 510–516.

Prajapati, R. K., Kumar, J. & Verma, S. (2013). *CrystEngComm* **15**, 9316–9319.

Presta, M., Rusnati, M., Belleri, M., Morbidelli, L., Ziche, M. & Ribatti, D. (1999). *Cancer Res*. **59**, 2417–2424.

Purohit, C. S. & Verma, S. (2006). *J. Am. Chem. Soc.* **128**, 400–401.

Purohit, C. S. & Verma (2007). *J. Am. Chem. Soc*. **129**, 3488–3489.

Rajabi, K., Gillis, E. A. L. & Fridgen, T. D. (2010). *J. Phys. Chem. A* **114**, 3449–3456.

Rao, C. N. R., Venkataraghavan, R. & Kasturi, T. R. (1964). *Can. J. Chem.* **42**, 36–42.

Redei, I., Green, F., Hoffman, J. P., Weiner, L. M., Scher, R. & O'Dwyer, P. J. (1994). *Invest. New Drug.* **12**, 319–321.

Rey, R., Ingrosso, F., Elsaesser, T. & Hynes, J. T. (2009). *J. Phys. Chem. A* **113**, 8949–8962.

Rigaku (2008–2015). *CrystalClear*, Rigaku Corporation, Tokyo, Japan.

Rother, I. B., Willermann, M. & Lippert B. (2002). *Supramol. Chem*. **14**, 189–197.

Senelaa, E., Yilmaz, V. T. & Harrison, W. T. A. (2005). *Z. Naturforsch. B* **60**, 659–662.

Sheldrick, G. M. (2015a). *Acta Cryst.* A**71**, 3–8.

Sheldrick, G. M. (2015b). *Acta Cryst.* C**71**, 3–8.

Shen, T. Y., McPherson, J. F. & Linn, B. O. (1966). *J. Med. Chem.* **9**, 366–369.

Sinha, I., Kösters, J., Hepp, A. & Müller, J. (2013). *Dalton Trans*. **42**, 16080–16089.

Sun, J., Wei, Y.-H., Liu, F.-L. & Sun, D. (2012). *RSC Adv.* **2**, 10189–10194.

Tjahjanto, R. T. & Beck, J. (2009). *Eur. J. Inorg. Chem.* **2009**, 2524–2528.

Venkatesh, V., Kumar, J. & Verma, S. (2011). *CrystEngComm* **13**, 6030–6032.

Verma, S., Mishra, A. K. & Kumar, J. (2010). *Acc. Chem. Res.* **43**, 79–91.

Volonté, C. & Greene, L. A. (1992). *J. Neurochem.* **58**, 700–708.

Wong, D. R., Coenen, M. J. H., Derijks, L. J. J., Vermeulen, S. H., van Marrewijk, C. J., Klungel, O. H., Scheffer, H., Franke, B., Guchelaar, H.-J., de Jong, D. J., Engels, L. G. J. B., Verbeek, A. L. M., Hooymans, P. M. & Team, T. R. (2017). *Aliment. Pharm. Ther*. **45**, 391–402.

Yamanari, K., Kida, M., Yamamoto, M., Fujihara, T., Fuyuhiro, A. & Kaizaki, S. (1996). *J. Chem. Soc., Dalton Trans*. pp. 305–309.

Zimmerman, T. P. & Elion, G. B. (1974). *Cancer Res.* **34**, 221–224.

Supporting information

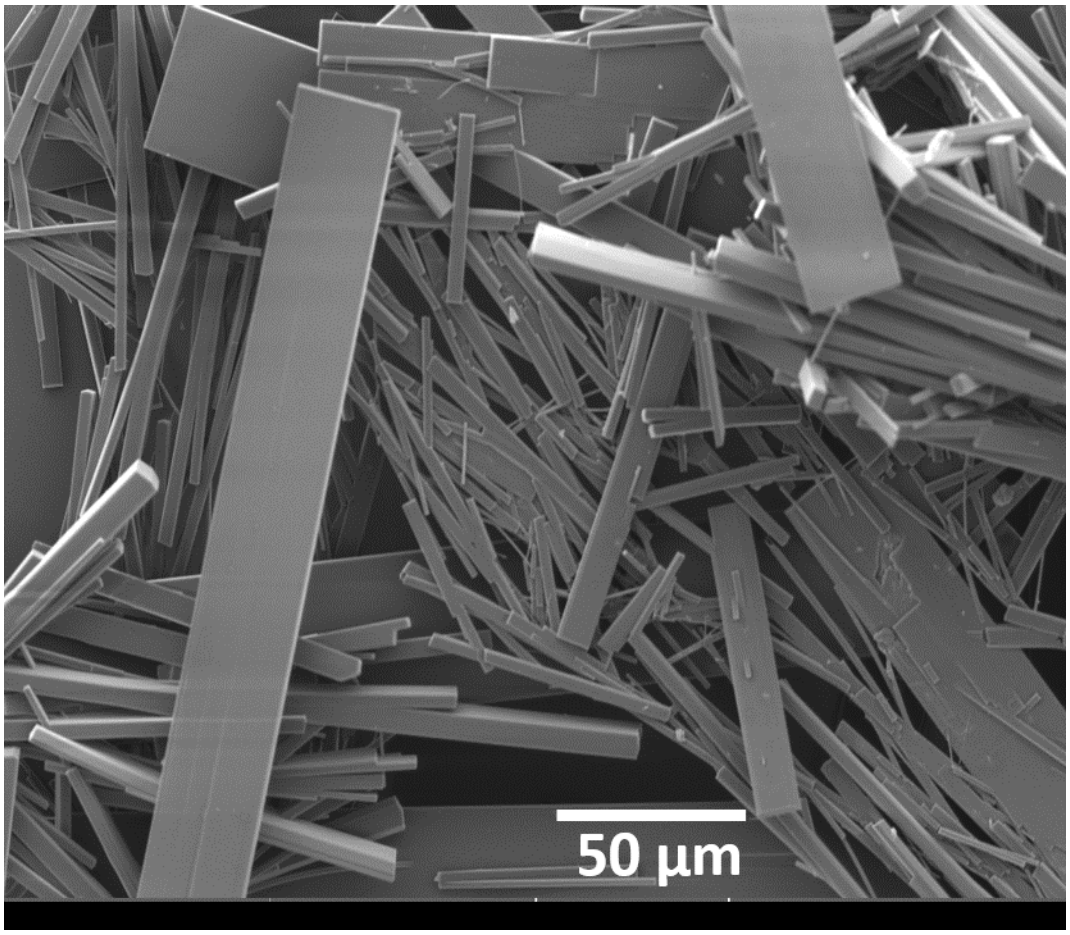

Figure S1 SEM image for the title complex.

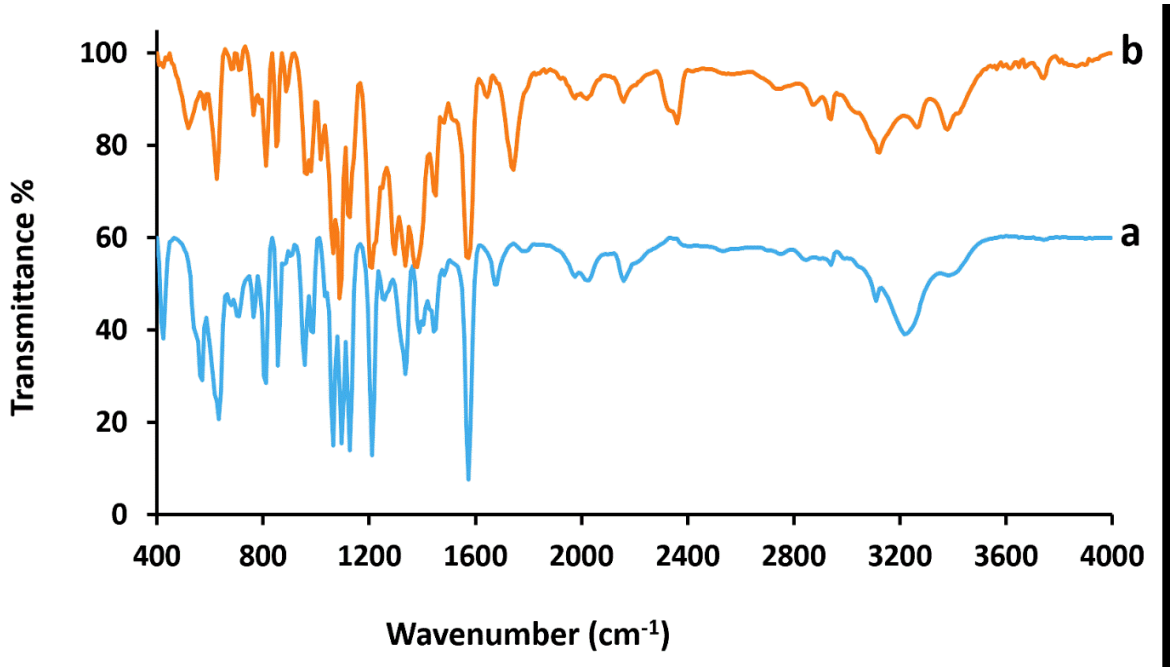

Figure S2 FTIR spectra of (a) 6-MMPR and (b) the silver complex.

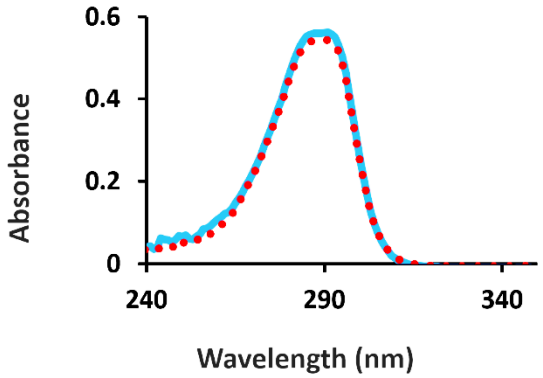

Figure S3 UV-Visible absorption spectra of 6-MMPR (blue) and its silver complex (red dots) in methanol solution (1×10^{-4} mol L^{-1}).